

# Development of Coated Ceramic Components for the Aluminum Industry

F. Jorge Lino, Teresa P. Duarte, and Ricardo Maia

(Submitted 12 November 2001; in revised form 4 February 2002)

In general, due to ceramic's high hardness, which makes machining operations extremely difficult and very expensive, ceramic components are formed in shapes very close to the final ones. Considering this, a manufacturing process, based on a sol-gel reaction that allows rapid production of ceramic components in the final shape with a low level of shrinkage was developed. Although the ceramics obtained presented good behavior in short-term contact with molten aluminum alloys, there was no guarantee that the components produced would have adequate continuous resistance to chemical and erosive wear by liquid metals. To enhance their resistance, the ceramic parts were coated by flame spray. Different powders and conditions were used to determine the degree of coating adhesion to the substrate. The coated specimens were then submerged in a molten aluminum bath, at different temperatures and time settings, to evaluate the interaction between the ceramic components and the molten aluminum alloys.

**Keywords** ceramic coatings, ceramic substrates, flame spray, foundry, sol-gel

## 1. Introduction

In general, due to ceramic's high hardness, which makes machining operations extremely difficult and very expensive, ceramic components are obtained in shapes very close to the final ones. A good alternative to produce ceramic components is based on a manufacturing process that uses a sol-gel reaction and cheap raw materials. This process converts models made by rapid prototyping techniques, such as stereolithography (SL), laminated object manufacturing (LOM), or other techniques, into ceramic components. The main purpose of the technique is to obtain ceramic parts for the foundry industry.<sup>[1-3]</sup> Figure 1 presents two of these ceramic components.

The ceramic components are produced by mixing, in variable proportions, a ceramic aggregate composed of faceted mullite particles [55 wt.% mullite ( $\text{Al}_2\text{O}_3 \cdot 2\text{SiO}_2$ ) and 45 wt.% amorphous silica], round zirconium silicate ( $\text{ZrSiO}_4$ ) particles, and faceted rutile ( $\text{TiO}_2$ ) particles of different sizes, and a liquid binder {tetraethoxysilane [ $\text{Si}(\text{OC}_2\text{H}_5)_4$ ]}.<sup>[1,2]</sup>

Using slurries of ceramic powders with different shapes, quantity, and chemical compositions, one can obtain ceramic components with variable characteristics, such as permeability to the gases coming from the liquid metal, mechanical strength, thermal conductivity, thermal expansion, surface roughness, and so on. A catalyst is added to the binder to start the sol-gel reaction. The liquid slurry is poured into a box with a cavity shaped like the component to be produced. After a short time, controlled by the amount of catalyst, the ceramic mixture ac-

quires a rubber consistency. After demolding from the pattern, the gelation reaction is stopped with ethyl alcohol and the component is ignited. After stabilization and burnout of binder volatiles, the ceramic component is sintered to generate an inert component with the desired strength for contact with commercial ferrous and non-ferrous alloys (more details about this process are indicated in references).<sup>[1,2-5]</sup>

Although the ceramic particles discussed have been frequently used in ceramic moldings for metallic mould production,<sup>[3-5]</sup> there is still no guarantee that the components produced will have adequate continuous resistance to chemical and erosive wear of the liquid metals. To further improve their resistance, flame sprayed ceramic coatings can be applied on the components surface.

The most significant thermal spray processes are plasma spraying, high velocity oxyfuel spraying (HVOF), arc wire spraying and flame spraying.<sup>[6]</sup>

**Table 1 Ceramic Slurry Characteristics**

Ceramic Powders	Binder and Ratio (Weight) Binder/Ceramic Powder	Catalyst Relative to the wt.% of the Binder
15 wt.% zircon -325 mesh (<45 $\mu\text{m}$ )		
30 wt.% zircon -200 mesh (<75 $\mu\text{m}$ )		
15 wt.% zircon sand (between 180 and 100 $\mu\text{m}$ )	Hydrolyzed	Ammonium
10 wt.% molochite 50/80 mesh (between 300 and 180 $\mu\text{m}$ )	tetraethoxysilane	hydroxide solution
10 wt.% molochite 30/80 mesh (between 600 and 180 $\mu\text{m}$ )	1/7	(at 2.5 wt.%)
10 wt.% molochite 16/30 mesh (between 1180 and 600 $\mu\text{m}$ )		1.5 wt.%
10 wt.% rutile -200 mesh (<75 $\mu\text{m}$ )		

**F. Jorge Lino, Teresa P. Duarte, and Ricardo Maia**, FEUP—Faculdade de Engenharia da Universidade do Porto, DEMEGI—Departamento de Engenharia Mecânica e Gestão Industrial, Rua Dr. Roberto Frias, 4200-465 Porto, Portugal. Contact e-mail: falves@fe.up.pt.

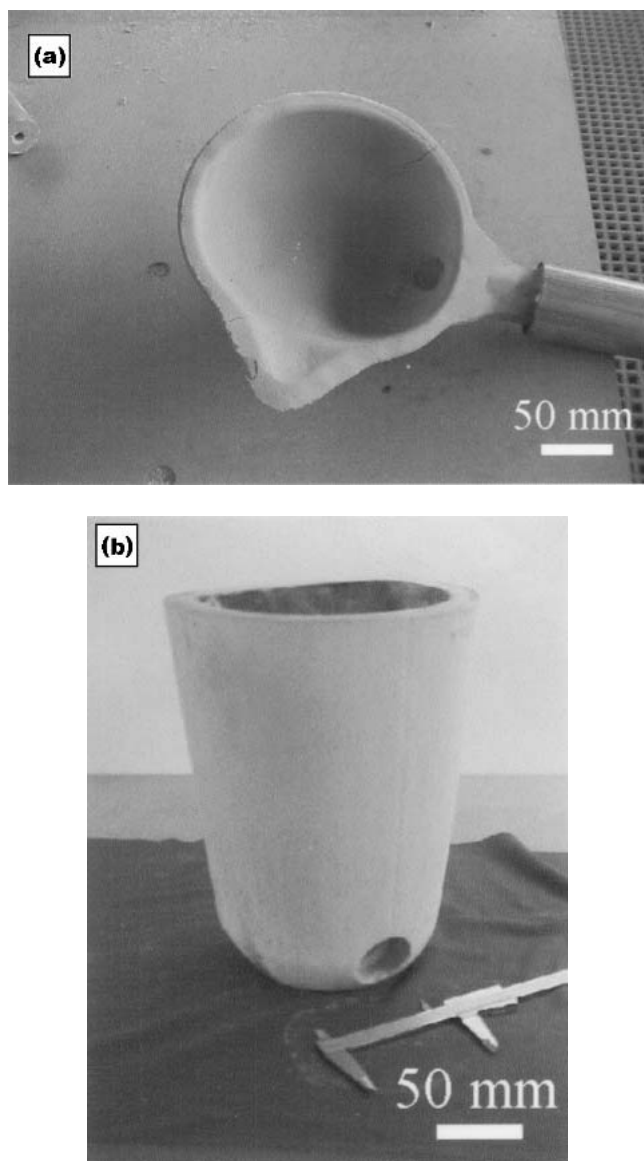


**Fig. 1** Ceramic components: (a) casting ladle and (b) crucible

The current study uses a flame spray gun. The flame spray process has spray hardware that is extremely versatile and user-friendly. It has a low initial cost and low maintenance requirements, but, when compared with other thermal spray coating processes, it produces lower coating adhesion. This process uses a mixture of oxygen and acetylene to form the flame, although it can also use hydrogen or propane as combustibles.

After the ignition of the combustible mixture, the coating material is added to the flame in a wire or a powder form. The combustion gas jet accelerates the coating material toward the substrate with or without the aid of a compressed air jet.<sup>[6]</sup>

Almost any kind of material that is stable at high temperatures can be sprayed, since it may not decompose, making it possible to be used in heat-treated components without modifying its metallurgical properties. The most significant disadvantage of the process is the fact that it can only coat in the line of sight, making it impossible to coat components with narrow

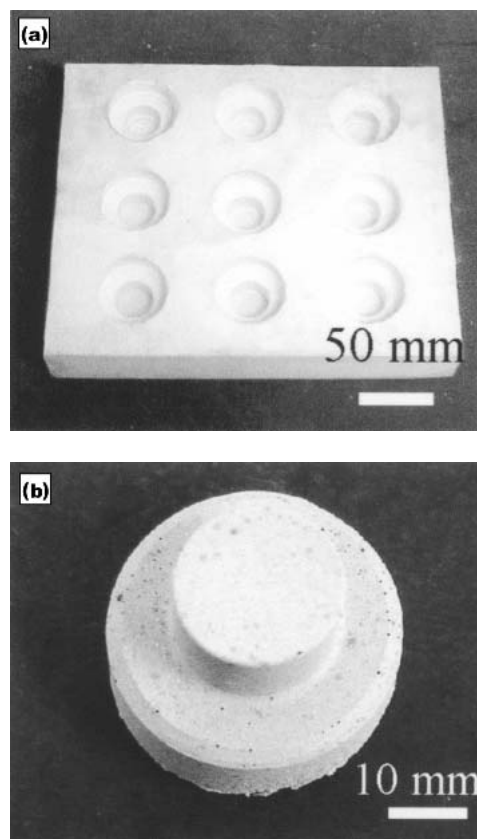


**Fig. 2** Ceramic test specimens: (a) silicon mould for 9 specimens for the adhesion test, (b) ceramic specimen based on the ASTM Standard C633-79<sup>[8]</sup>

holes. Its typical applications are wear elimination, dimensional recovery of worn components, biomaterial coatings, polymeric and composite coatings, anti-corrosion applications, and thermal barriers, with the latter being the object of this study.<sup>[6,7]</sup>

## 2. Experimental Procedure

To produce the specimens necessary to characterize the tensile adhesion between the coatings and the substrate, a silicone mold was made. The specimens were produced based on the ASTM Standard C633-79.<sup>[8]</sup> A ceramic slurry, consisting of ceramic particles of different sizes of molochites, zircon, and rutile, a liquid binder (tetraethoxysilane) and a catalyst (ammonia) (see Table 1), was poured into the silicone mould for gelation. After demolding and ignition, the ceramic specimens were sintered at 1500 °C for 2 h to achieve high mechanical strength (for the experimental details, see Ref. 1). Figure 2 presents the silicone mould and one of the test specimens obtained (with a 23.5 mm facing diameter for coating. Specimens have a 25 mm diameter, but during sintering they suffer 6% shrinkage). The geometry of these specimens is different from the one specified in the ASTM Standard C633-79<sup>[8]</sup> due to the fact that was impossible to obtain a threaded ceramic specimen.

To have good adhesion of the coating to the substrate, it is generally claimed that the parts should have a certain surface

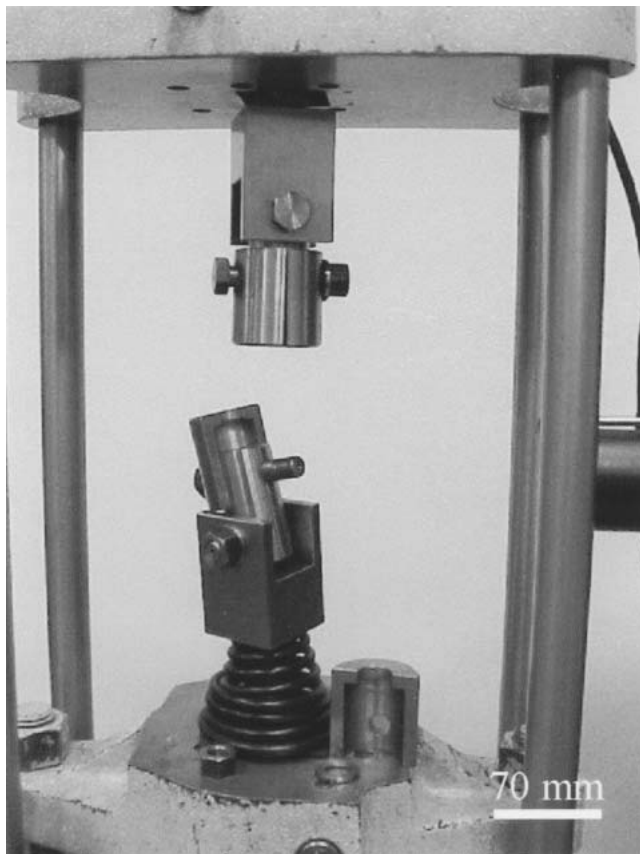


**Fig. 3** Apparatus for the tensile tests mounted in a universal Tinius Olsen tensile machine (300 kN maximum load capacity); the tests were performed at 0.016 mm/s speed.

**Table 2** Properties of the Metco Powders<sup>[9]</sup>

Powders	101 NS	210 NS-1	447 NS Bond Coat
Chemical Composition	94 wt.% Al <sub>2</sub> O <sub>3</sub> 2.5 wt.% TiO <sub>2</sub> 2.0 wt.% SiO <sub>2</sub> 1.0 wt.% FeO 0.5 wt.% Others	24 wt.% MgO 76 wt.% ZrO <sub>2</sub>	5 wt.% Mo 5.5 wt.% Al 89.5 wt.% Ni
Particle Dimension, μm	5-45	10-53	45-88
Melting Point, °C	2 010	2 140	660

**Table 3** Spray Characteristics

Set	Metco Powder Reference <sup>[9]</sup>	Coating Thickness	Spraying Time, s	Substrate Preheating Time, s
1	101 NS	Thin	3	5
2	101 NS	Thick	6	5
3	447 NS/101 NS	Thin + thin	1.5 + 3	5
4	101 NS	Thin	3	5
5	447 NS/101 NS	Thin + thick	1.5 + 6	5
6	210 NS-1	Thick	6	5
7	447 NS/210 NS-1	Thin + thin	1.5 + 3	5

A thick coating was defined as the one obtained by doubling the spraying time used for a thin coating, which is 3 s. It should also be mentioned that due to the high deposition rate of the 447 powder, this powder was only sprayed for 1.5 s.

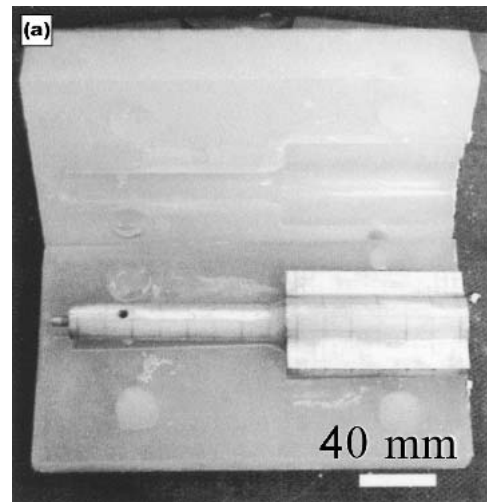


**Fig. 4** Prototype for the reaction tests: (a) LOM prototype in the silicone mold and (b) coated ceramic component

roughness.<sup>[6]</sup> Although this is true for metals, with this type of ceramics this was not necessary because they were already rough enough. When the surface roughness was increased (by gluing a SiC paper #80 on the patterns over which the silicone was cast), the adhesion strength of the coating to the substrate was significantly reduced. In fact, when the roughness increases, ceramic particles on the surface do not have a high number of contacts with the rest of bulk materials, and consequently they are easily detached from the substrate. Considering this, the ceramic surface roughness obtained after demolding from the silicone mould was kept constant [medium surface roughness (Ra) around 11 μm] for all substrates.

Seven sets of ten specimens each were coated by flame spray (Gun 5P-II, Metco Perkin Elmer, Westbury, NY) using three different powders, which were selected in accordance with technical information<sup>[9]</sup> and considering the coating resistance to molten aluminum alloys.<sup>[4,7]</sup> Table 2 presents the most relevant properties of these powders, while in Table 3 are indicated the main spray characteristics.

In this study, a thick coating was defined as the one obtained by doubling the spraying time used for a thin coating, which is 3 s. It should also be mentioned that due to the high deposition rate of the 447 NS powder, this powder was sprayed for only 1.5 s. Other spraying parameters, such as spraying distances (65-180 mm), metering valve (Ref. 15 for 447 NS and Ref. 12 for the others) and nozzle type (P7-G), flux (acetylene  $0.3 \times 10^{-3}$  m<sup>3</sup>/s,

oxygen  $0.45 \times 10^{-3} \text{ m}^3/\text{s}$  for 447 NS powder and  $0.5 \times 10^{-3} \text{ m}^3/\text{s}$  for the others) and gas pressures (acetylene pressure 0.1 MPa, oxygen pressure 0.21 MPa for 447 NS powder, and 0.17 MPa for the others), were the ones recommended by the manufacturer (Metco Perkin Elmer, Westbury, NY).

Test specimens were glued with a cyanoacrylate adhesive (C15, AXSON Iberica Composites/S.A., Barcelona, Spain) to a polished (with #800 SiC paper) uncoated aluminum specimen inside a sleeve, to avoid shear stresses. Specimens were left 24 h, at room temperature, with a 3 kg weight on the top, for drying the

**Table 4 Test Parameters**

Specimen (component) Ref.	Temperature, °C	Time, h	Rotating Speed, rpm	Coating	Comments
1	700	3	16.8	Without Coating	...
2	700	24	16.8	Without Coating	...
3	700	168	16.8	447 NS + NS 101	...
4	800	168	33.6	Set 2 – NS 101	Specimen broken after 4 days of test
5	800	168	26	Set 5	...
6	800	168	26	447 NS + NS 101	...
7	800	168	26	Without coating	Presented
8	800	168	26	Set 2 – NS 101	Manufacturing defects
				Set 2 – NS 101	...

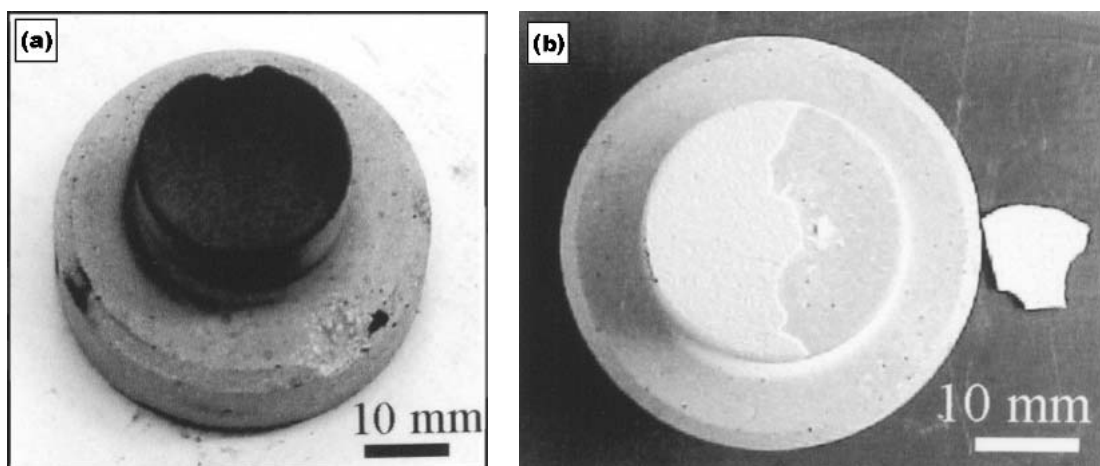


**Fig. 5** Ceramic test specimens with coatings: (a) 101 NS powder, (b) 210 NS-1 powder (Set 6) presenting a bad adhesion to the substrate

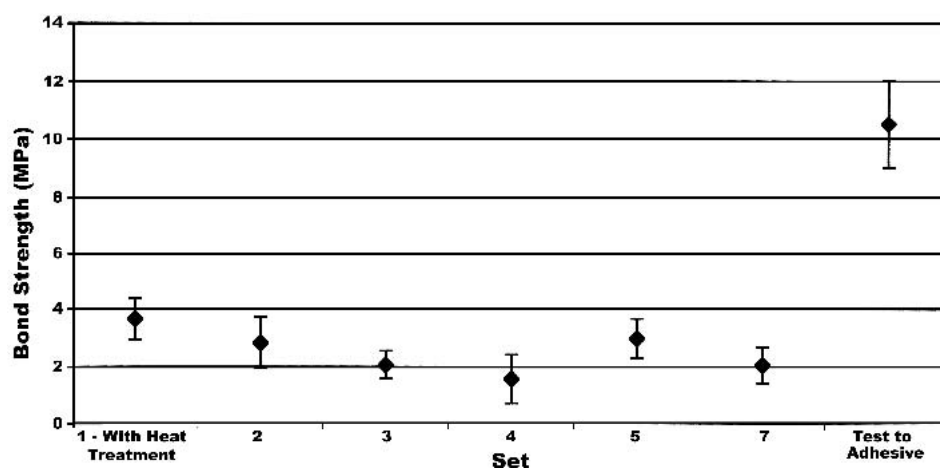


**Fig. 6** Bond strength for the different sets (ten specimens each) tested

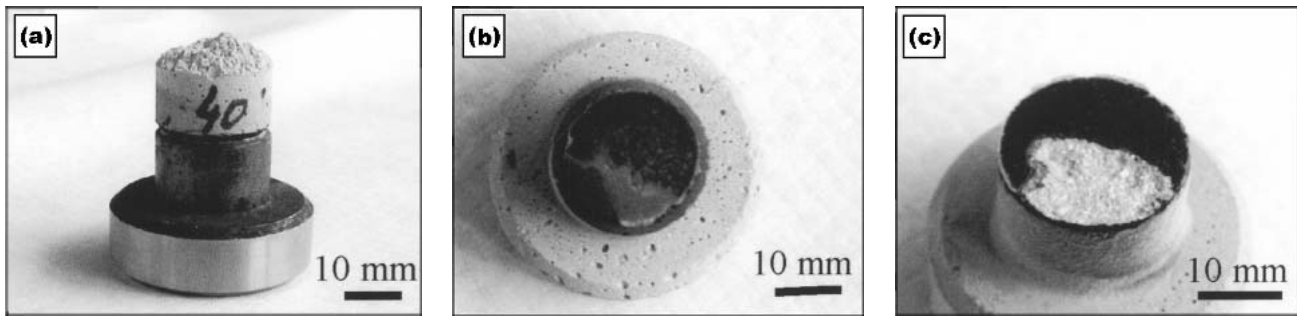


Fig. 7 Test specimen fracture: (a) cohesive fracture of the substrate, (b) fracture at the glue level, and (c) mixed type

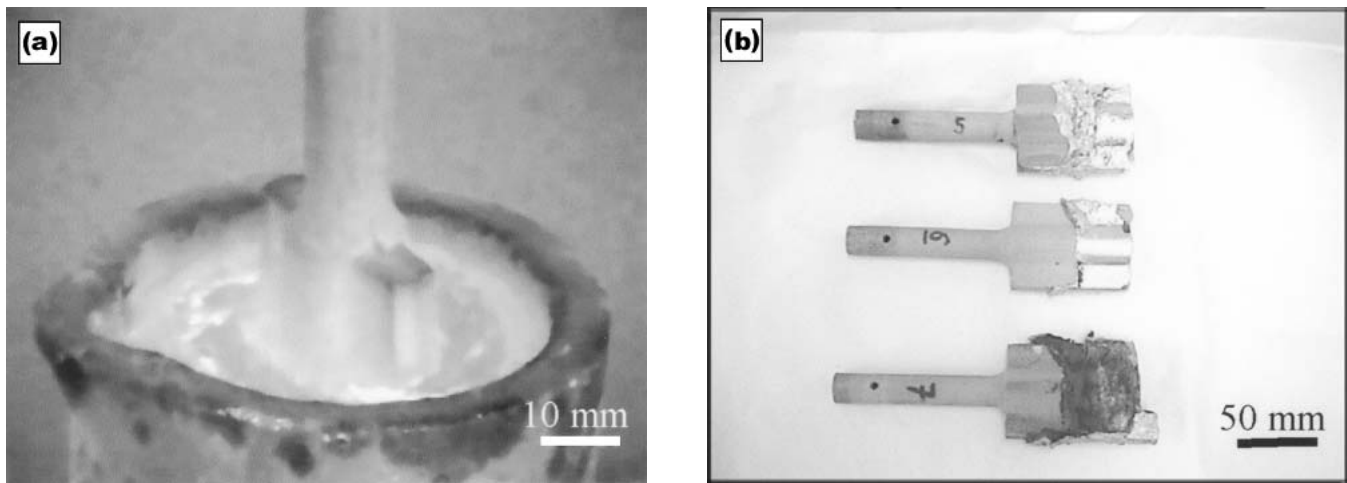


Fig. 8 Reactivity test: (a) specimen during the test and (b) 3 specimens after the test

adhesive. The specimens were then placed inside the apparatus shown in Fig. 3 and tensile tested, at room temperature, in a universal Tinius Olsen tensile machine (Willow Grove, PA, 300 kN maximum load capacity) with 0.016 mm/s speed.

One set with just metallic specimens was also prepared and tested to determine the glue strength.

### 2.1 Molten Aluminum Reaction Tests

For the reaction tests with molten aluminum alloys, a special furnace was designed and manufactured. The objective of this test is the evaluation of the erosive and reaction behavior of the ceramic component in a real environment and in a continuous situation.<sup>[10]</sup> A ceramic test specimen component for the tests was first modeled with the aid of CAD 3D software, and then a LOM prototype was obtained. Figure 4 presents the LOM prototype, after the finishing operations, in the silicone mold used to cast 8 ceramic parts, and a coated ceramic component. Ceramic parts were then sintered at 1500 °C for 2 h.

The ceramic parts were attached to a spinning shaft and submerged into a molten aluminum bath. The reaction tests were performed submerging coated and uncoated ceramic parts in a molten aluminum alloy (AFNOR AS7G, chosen because is a very common foundry aluminum alloy) bath. Test parameters are shown in Table 4.

The shaft rotates relative to the crucible containing the aluminum alloy, which promotes a dynamic contact between the aluminum and the ceramic component to be tested.

The first four tests were performed to set up the right experimental conditions (amount of aluminum inside the crucible, speed, and test temperature). It should be mentioned that the tests were performed without controlled atmosphere, which allowed the formation of a surface layer of aluminum oxide on the aluminum bath and around the shaft.

After the tests, all the components were analyzed using optical and electronic microscopy.

## 3. Results and Discussion

Figure 5 presents two coated specimens. Set 6 (powder 210 NS-1, see Table 2) was not tested because, when applied without the bond coat 447 NS, it peels off very easily (see Fig. 5b).

The results obtained with the tensile tests performed on the coated ceramic specimens are indicated in Fig. 6. Sets 1 and 4 were sprayed under the same conditions. However, Set 1 was subjected to a subsequent heat treatment. In fact, Kishitake and co-authors<sup>[11,12]</sup> claim that a subsequent heat treatment at 1000

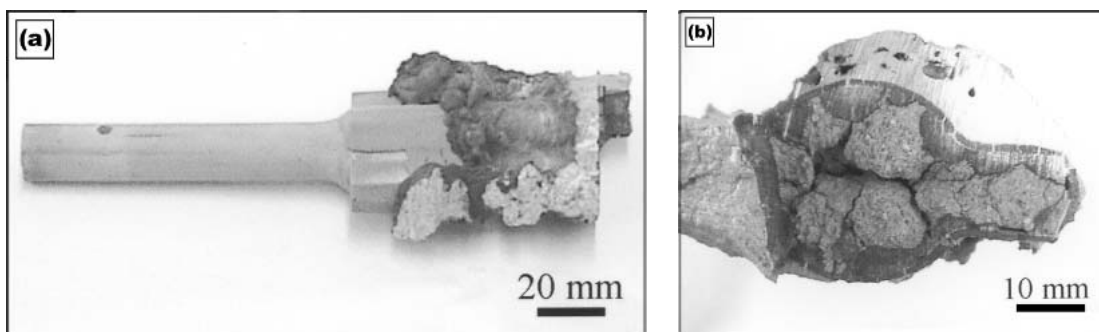


**Fig. 9** Component 7 with manufacturing defects after the test

°C for 2 h can improve the adhesion of the coating to the substrate.

As one can see, the highest tensile bond strengths, around 3 MPa, are obtained with alumina thick coatings, with or without bond coat (sets 2 and 5).

The heat treatment (set 1) increased the bond strength by 2 MPa, relatively to the as-sprayed thin coating of the same material (set 4). Comparing sets 1 and 2, which have similar bond strengths for thin and thick alumina coatings, respectively, it seems that there is no reason to choose to heat treat as was done for set 1. In fact, heat treatment increases the production time and the cost without significant improvement of the bond strength. Considering this, in a first step, only sets 2 and 5 were selected for the reaction tests.

The dispersion in the bond strength values is probably a result of the sensitivity of these tests to the porosity and other microstructural defects present in the ceramic components. Figure 7 presents three types of fracture detected in the test specimens. Sets 2 and 5 present essentially a cohesive fracture of the substrate, while sets 1, 3, and 4 exhibit all the three types of fracture, with no special incidence in one specific type of failure. Set 7 shows preferentially failure with coating decohesion from the substrate.

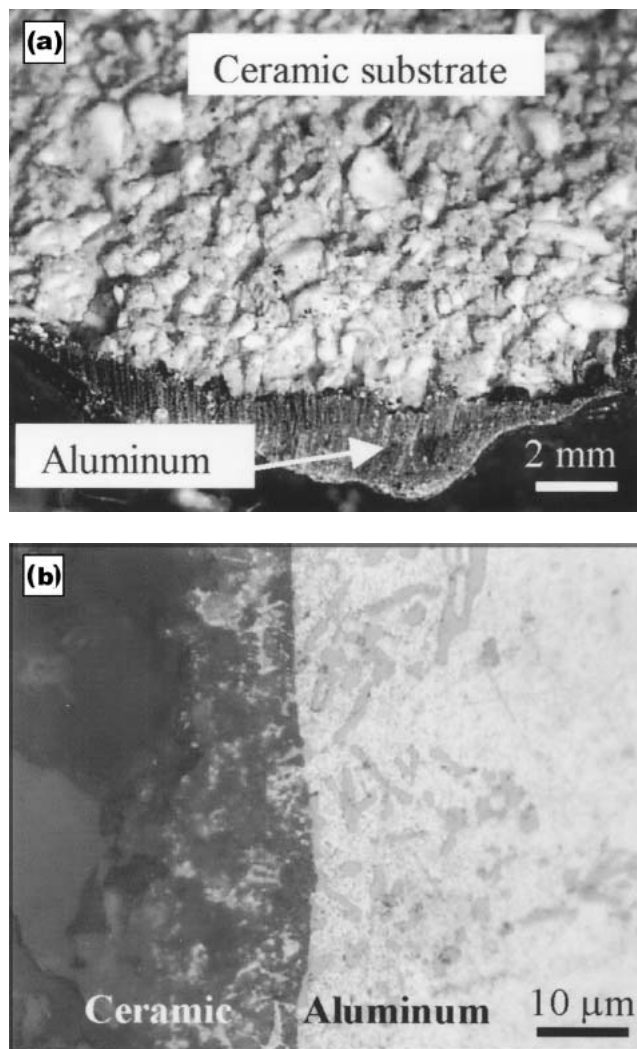
For the reaction tests, some of the parts were coated using the parameters specified for sets 2 and 5, while the others were left uncoated.

Figure 8 shows one coated specimen during and after the reactivity test, respectively.

During the test, the viscosity and thickness of the aluminum oxide layer increases, generating an opposite torque in the shaft. This is the reason for the fracture observed in specimen 4, which was tested at high rotating speeds.

Specimen 7 presented manufacturing defects, which promoted aluminum infiltration in the ceramic and the rapid destruction of the component, as one can see in Fig. 9.

Components without coatings showed aluminum penetration with the aluminum layer stuck to the ceramic substrate, as one can see in Fig. 10 and 11. In fact, Fig. 10(b) shows very well this penetration in the interface: aluminum (on right, lighter region)-ceramic substrate (on left, black region). Close to the interface, on the ceramic side, one can see lighter regions that are a consequence of the aluminum penetration in the ceramic substrate. Figure 11 presents a backscattered SEM micrograph of the interface and the x-ray spectrum obtained on the ceramic (left side). As one can see, there is a formation of aluminum oxide on the ceramic surface. This aluminum penetration makes



**Fig. 10** Component 2 without coating: (a) at low magnification (image obtained in a scanner), (b) at high magnification (optical micrograph) showing the ceramic substrate (on the left) with aluminum (on the right) penetration (lighter regions below the dark regions); the darker regions on the aluminum side represent primary silicon crystals and eutectic silicon.

difficult the detachment of the aluminum layer stuck to the ceramic.

X-ray analysis did not detect the formation of other phases in

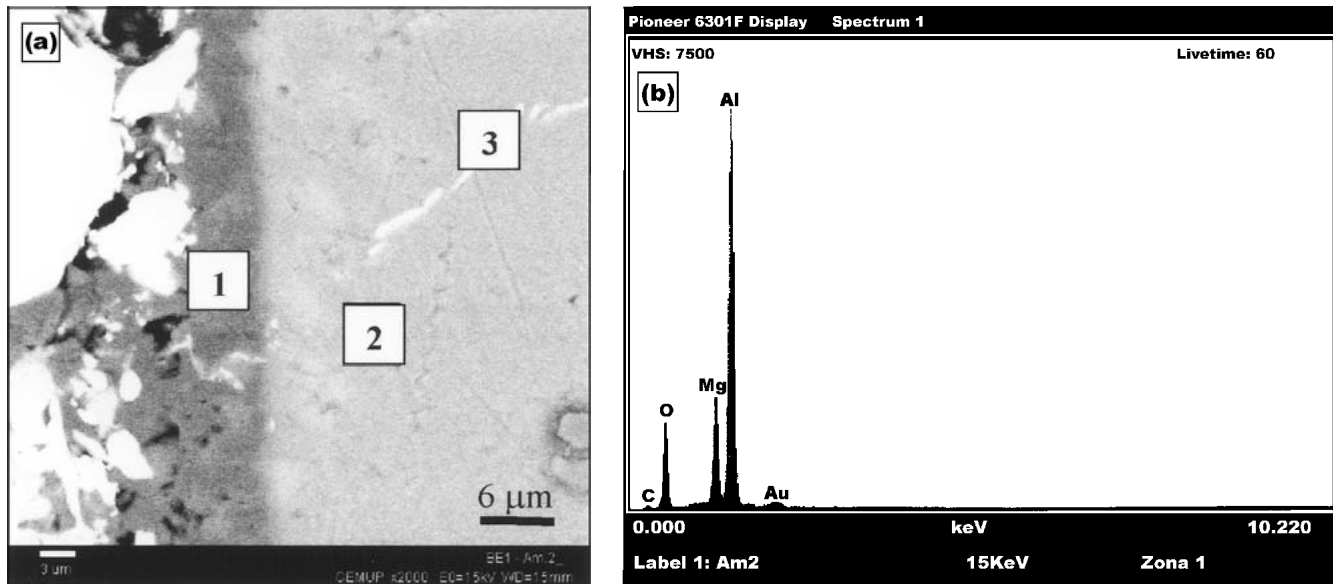


**Fig. 11** Component 2 without coating: (a) backscattered SEM micrograph showing the aluminum penetration on the ceramic substrate (on left), (b) x-ray spectrum obtained in point 1 of (a). Points 2 and 3 represent regions with high aluminum content (aluminum compounds formation characteristics of AS7G aluminum alloys).

the interface than the aluminum oxide (alumina). On the other hand, in the coated components with thick alumina coatings, the aluminum layer detaches very easily from the shaft (see Fig. 12 and 13). Figure 13(a) shows that the resin used during the materialographic sample preparation for microscopic analysis penetrated in the free space existing in the interface coating-aluminum. Figure 13(b) shows part of the aluminum layer detached from the coating.

The coating thickness was measured in some samples. The median values obtained were 290  $\mu\text{m}$  for the bond coat (447 NS) and 435-1300  $\mu\text{m}$  for the alumina coating (101 NS). The dispersion of the alumina coating thickness is due to the manual projection in ceramic substrates.

The results obtained demonstrate the benefit in coating the ceramic components for continuous or prolonged contact with aluminum alloys. In principle, any advantage was found in using a bond coat on these types of ceramics. This coating is useful in coating metals with ceramics, to overcome the thermal expansion mismatch between the two groups of materials. In this case, where the two groups have similar thermal expansion coefficients, this is not relevant.

#### 4. Conclusions

Ceramic components with tailored resistance for contact with a liquid aluminum alloy were developed. These ceramics were produced by a sol-gel process and sintered at 1500  $^{\circ}\text{C}$  for 2 h. In continuous contact with an AS7G (AFNOR) aluminum alloy, these ceramics tended to degrade by liquid penetration, but when coated with an alumina coating, they showed very good performance for short and long periods of time, with no aluminum penetration being observed. The coatings produced have around 3 MPa bond strength.

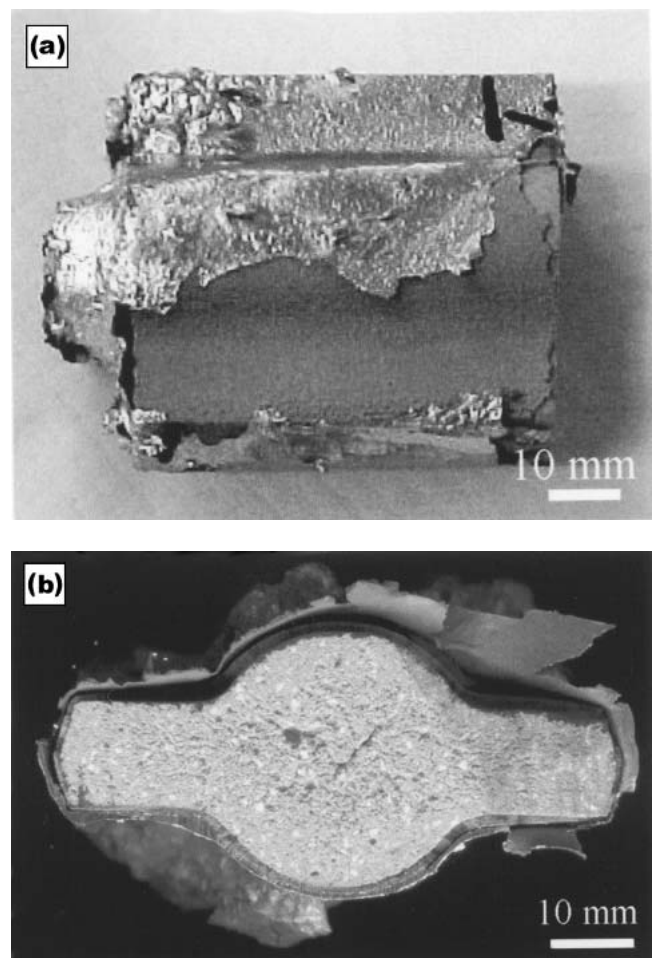


**Fig. 12** Components with thick alumina coatings: (a) component 4 and (b) component 8

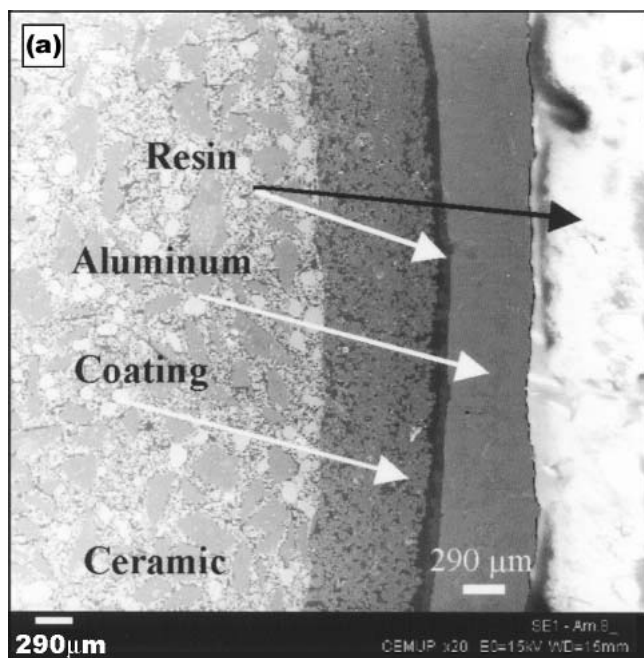


**Fig. 13** Component 8 with thick alumina coating: **(a)** SEM micrograph showing the different regions of the component (from left to right, ceramic substrate, thick alumina coating, resin, aluminum resolidified and resin). The lighter region on the right (resin) results from surface charging and **(b)** aluminum layer easily removed from the shaft presenting an unaffected coating by the reaction test.

## Acknowledgments

The authors acknowledge the financial support of FCT through PRAXIS XXI program of the Portuguese Government, Project PRAXIS/P/CTM/14145/98, "Study of Paintings, Coatings and Ceramic Components for Aluminum Foundry Industry."

## References

1. F. Jorge Lino Alves, T.P. Duarte, and J. Teixeira: "Manufacturing Ceramic Components With High Fracture Strength," *7<sup>as</sup> Jornadas de Fractura*, Universidade da Beira Interior, Covilhã, Portugal, 16-18 Feb 2000, pp. 248-54 (in Portuguese).
2. F. Jorge Lino Alves, F. Jorge Sousa Braga, M. São Simão, R. Jorge de Lemos Neto, and Teresa M.G.P. Duarte: "Protoclick—Rapid Prototyping," *Protoclick*, Porto, Portugal, Feb 2001 (in Portuguese).
3. T.P. Duarte, F. Jorge Lino, and R.L. Neto, "Ceramic Materials for Casting Metallic Molds," *Struers J. Mater. Struct.*, 1999, 34, pp. 9-11.
4. Anon: "Casting," in *ASM Handbook*, Vol. 15, ASM International, Materials Park, OH, 1988, pp. 248-52.
5. H.X. Ping: "Precision Cast Dies Produced by a Ceramic Mould Process—a Review," *Cast Metals*, 1989, 2(1), pp. 16-19.
6. L. Pawlowski: *The Science and Engineering of Thermal Spray Coatings*, John Wiley & Sons, New York, NY, 1995.
7. H. Herman and S. Sampath: *Thermal Spray Coatings*, The Thermal Spray Laboratory, Department of Materials Science and Engineering, State University of New York, Stony Brook, NY, <http://dol1.eng.sunysb.edu/tsl/thermal/article1.html>.
8. Anon: "ASTM Designation C633-79—Standard Test Method for Adhesion or Cohesive Strength of Flame-Sprayed Coatings" in *1989 Annual Book of ASTM Standards*, Section 2, Non Ferrous Products, Vol. 2.05, Metallic and Inorganic Coatings, Metal Powders, Sintered P/M Structural Parts, American Society for Testing and Materials, Philadelphia, PA, 1989, pp. 633-67.
9. Anon: Technical Bulletin—Flame Spray Equipment and Supplies, METCO 101 NS, METCO 447 NS, METCO 210 NS-1, Metco Perkin Elmer, Welsbury, NY, 1982.
10. M. Foulletier and D. Gold: "Selective, Accelerated Test for Evaluation of Refractory Lifetime in Contact With Aluminum Alloys," *UNITECR '91, 2nd Biennial Worldwide Conference on Refractories*, 2nd ed., German Refractories Association & Institut für Gesteinshüttenkunde, Stahleisen, Germany, 1992.
11. K. Kishitake, H. Era, F. Otsubo, and T. Sonoda: "Improvement of the Adhesion of Ceramic Coating on a Ceramic Substrate," *J. Therm. Spray Technol.*, 1998, 7(1), pp. 64-70.
12. K. Kishitake, H. Era, F. Otsubo, and T. Sonoda: "Ceramic Coating on a Ceramic With Metallic Bond Coating," *J. Therm. Spray Technol.*, 1997, 6(3), pp. 368-72.